Supporting Information

Hydrothermally derived p-n MoS_2-ZnO from p-p MoS_2-ZIF-8 for efficient detection of NO_2 at room temperature

Muhammad Ikram,[a, b] He Lv,[c] Zhuo Liu,[c] Keying Shi,*[c] Yongxiang Gao*[a, b]

[a]Institute for Advanced Study, Shenzhen University, Nanhai Avenue 3688, Shenzhen 518060, People's Republic of China. E-mail: yongxiang.gao@szu.edu.cn

[b]College of Physics and Optoelectronic Engineering, Shenzhen University, 518060 Shenzhen, People's Republic of China

[c]Key Laboratory of Functional Inorganic Material Chemistry, Ministry of Education. School of Chemistry and Material Science, Heilongjiang University, Harbin, 150080, P. R. China. E-mail: shikeying2008@163.com

Table of contents

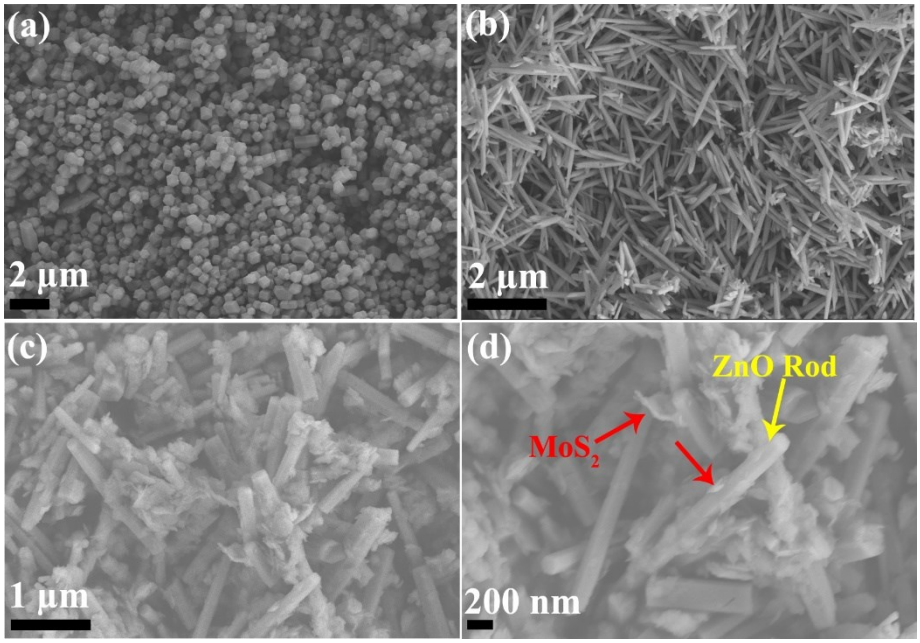

Figure S1. SEM images of (a) pure ZIF-8; (b) pure ZnO rods; and (c, d) MZR heterostructure

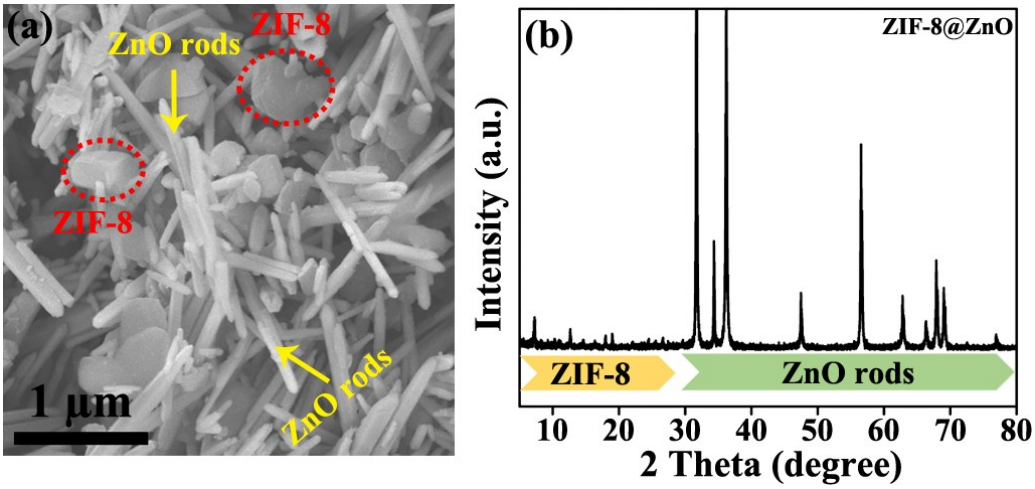

Figure S2. (a, b) SEM and XRD of ZIF-8@ZnO composites which was heating at 120 °C/2h hydrothermally.

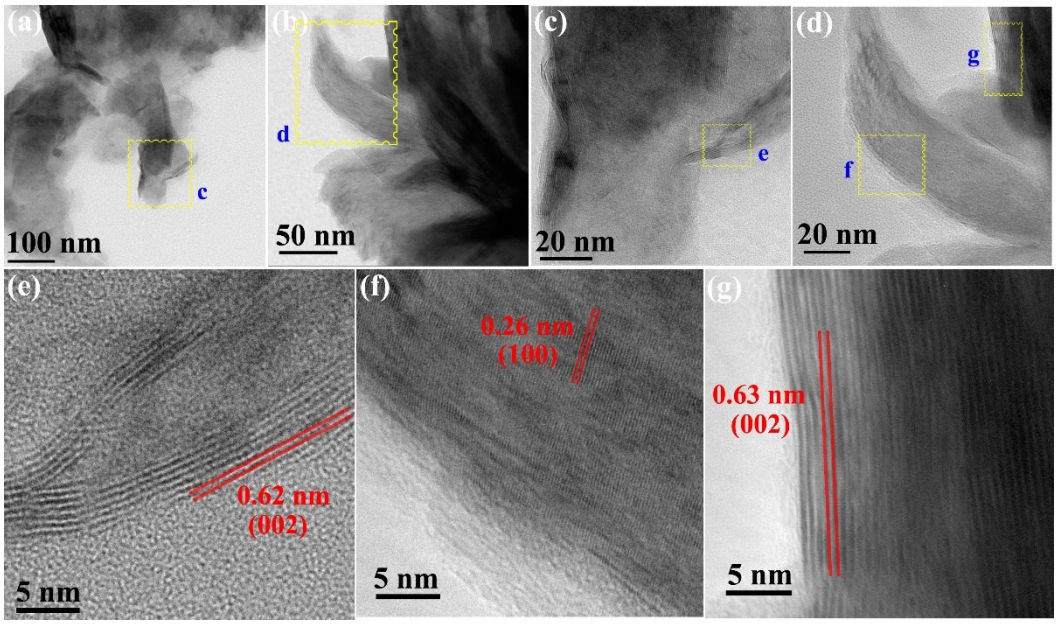

Figure S3. (a-d) TEM images; (e-g) HRTEM images of pristine MoS_2 NSs.

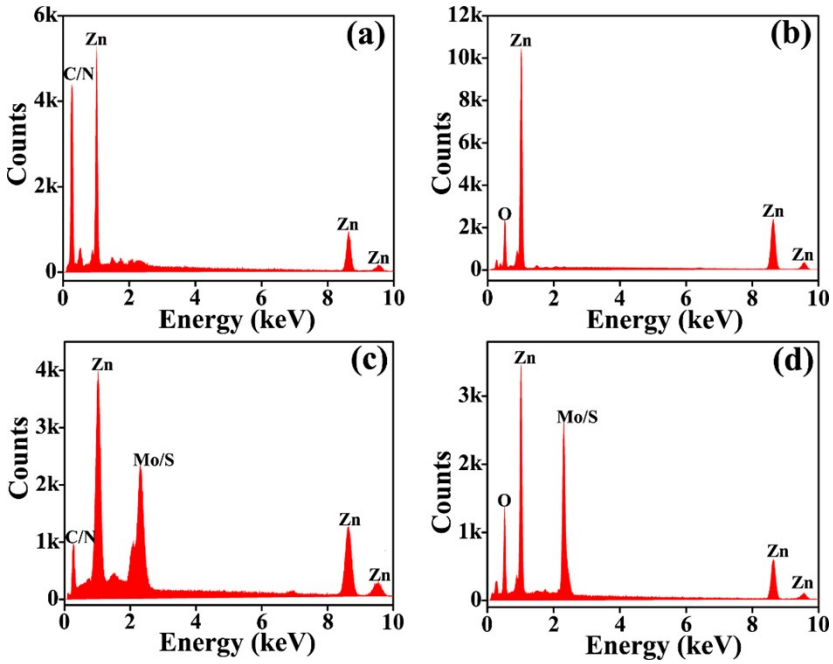

Figure S4. EDS spectra of (a) pure ZIF-8; (b) pure ZnO rods; (c) MoS_2@ZIF-8; (d) MoS_2@ZnO heterostructure.

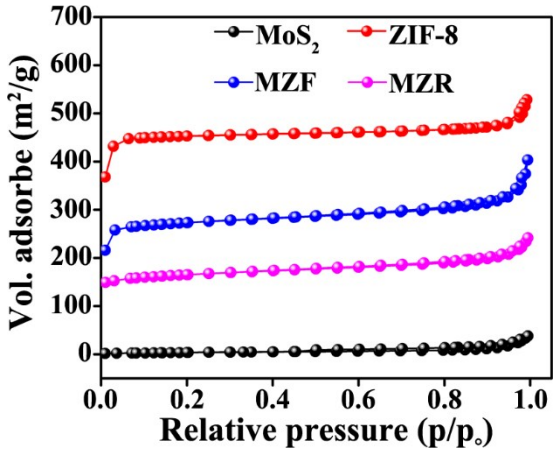

Figure S5. N_2 adsorption-desorption isotherms of the samples; the changes in the starting values in the y-axis for MoS_2, MZR, MZF, and ZIF-8 are 1.7, 147, 213, and 365 m^2/g respectively.

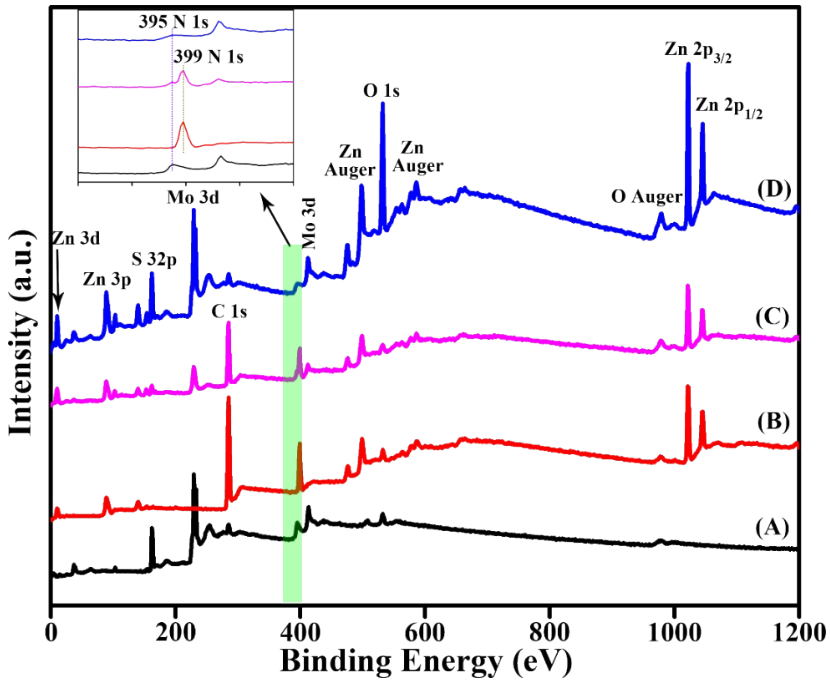

Figure S6. XPS survy spectra of MoS_2 (A), ZIF-8 (B), MZF (C), MZR (D); Insert figure shows that there are two N 1s peaks, one at 395 eV and one at 399 eV. The first one is due to the adsorption of N_2 gas on the surface of MoS_2 as it was heated at 600 °C/4h under nitrogen atmosphere, while the second is due to the ligant nitrogen only in pure ZIF-8 and MZF, which was eliminated after heating at 150 °C in MZR.

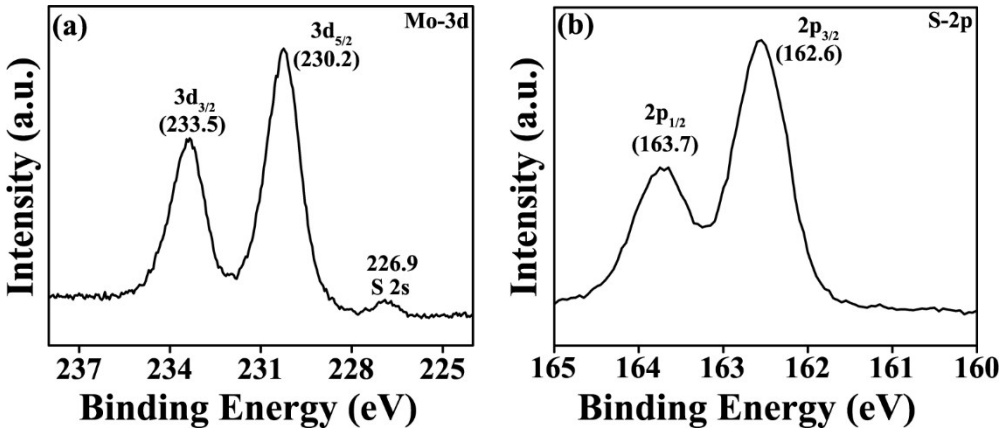

Figure S7. High resolution XPS spectra of Mo, and S of the pure MoS_2 NSs.

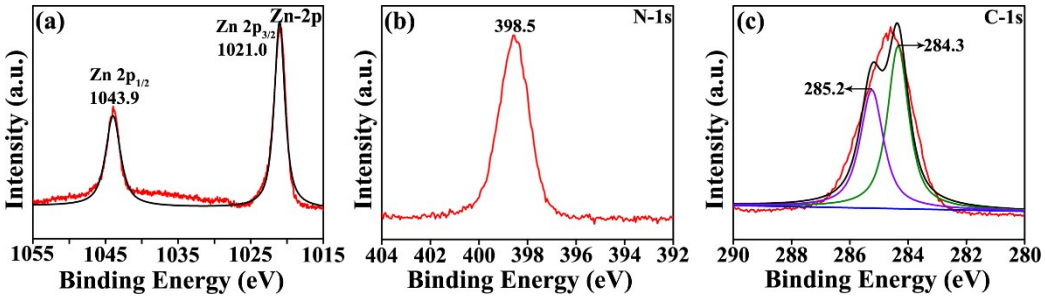

Figure S8. High resolution XPS spectra of pure ZIF-8; (a) Zn 2p, (b) N 1s, (c) C 1s.

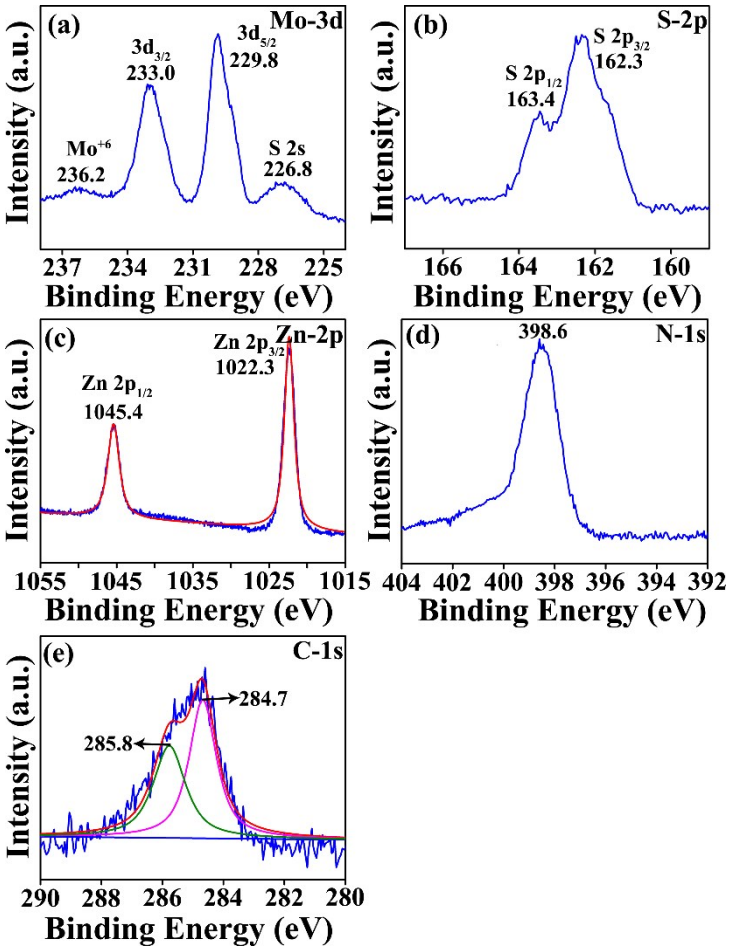

Figure S9. High resolution XPS spectra of MZF heterostructure; (a) Mo 3d, (b) S 2P, (c) Zn 2p, (d) N 1s, (e) C 1s.

Table S1. Comparative XPS Peak position of the pure MoS_2, ZIF-8 with MZF and MZR composites.

	Binding Energy (eV)		
Samples	Mo ($3d_{3/2}/3d_{5/2}$)	S ($2p_{1/2}/2p_{3/2}$)	Zn ($2p_{1/2}/2p_{3/2}$)
MoS_2	233.5/230.2	163.7/162.6	---/---
ZIF-8	---/---	---/---	1043.9/1021.0
MZF	233.0/229.8	163.4/162.3	1045.4/1022.3
MZR	232.8/229.6	163.5/162.4	1045.1/1022.0

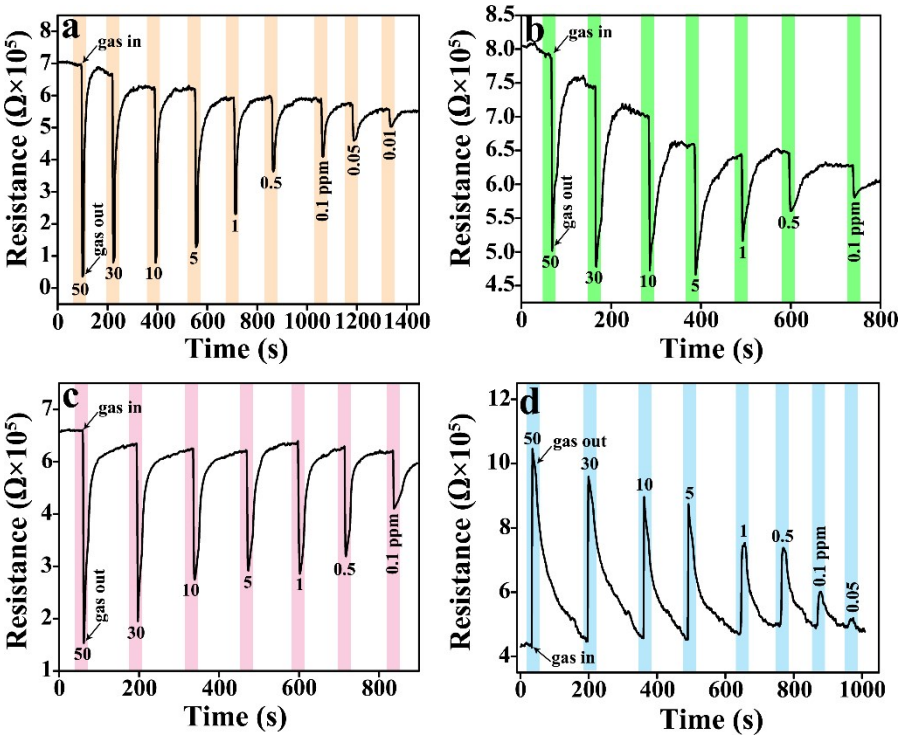

Figure S10. Dynamic response transient of (a) MZF; (b) pure MoS_2; (c) pure ZIF-8; (d) pure ZnO rods.

Table S2. Response and response/recovery times in seconds all of the sensors towards NO_2 gas at RT.

Sensors	**MoS_2**			**ZIF-8**			**ZnO**			**MZR**			**MZF**		
NO_2 (ppm)	**R**	t_{res}	t_{rec}	**R**	t_{res}	t_{rec}	**R**	t_{res}	t_{rec}	**R**	t_{res}	t_{rec}	**R**	t_{res}	t_{rec}
50	1.58	3.2	41.0	3.65	2.8	50.6	5.06	3.1	86.4	**34.91**	**1.5**	**30.9**	19.56	2.1	40.9
30	1.52	3.8	39.4	2.74	4.3	49.6	3.14	3.5	83.8	**31.27**	**1.9**	**28.8**	8.35	3.0	35.7
10	1.48	4.6	35.7	2.15	5.8	50.1	2.44	4.7	75.2	**29.52**	**2.1**	**25.6**	7.81	3.6	34.3
5	1.37	5.8	33.1	1.77	6.3	42.1	2.29	6.1	69.3	**24.85**	**3.2**	**22.4**	4.86	5.3	29.7
1	1.24	7.2	30.1	1.88	8.2	40.5	1.63	7.0	55.2	**9.49**	**4.8**	**18.0**	2.55	6.2	21.3
0.5	1.15	7.9	26.2	1.65	8.7	38.9	1.51	8.1	47.4	**4.57**	**6.3**	**16.5**	1.64	7.1	18.8
0.1	1.08	11.4	21.4	1.25	10.4	35.7	1.18	9.9	41.6	**1.67**	**8.0**	**15.4**	1.44	9.5	15.9
0.05							1.04	11.3	24.9	**1.41**	**8.6**	**13.3**	1.24	10.3	14.2
0.01										**1.05**	**11.2**	**10.2**	1.01	12.6	12.6

R-Response t_{res}-response time in seconds t_{rec}-recovery time in seconds

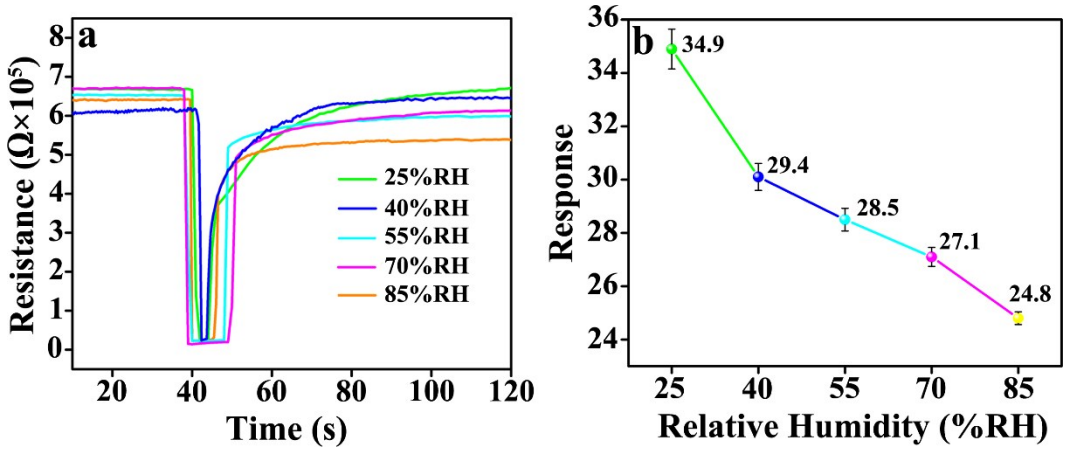

Figure S11. (a) Dynamic response transient of MZR to 50 ppm NO_2 at different relative humidity (RH) at RT; (b) Response of the sensor corresponding to Figure (a).

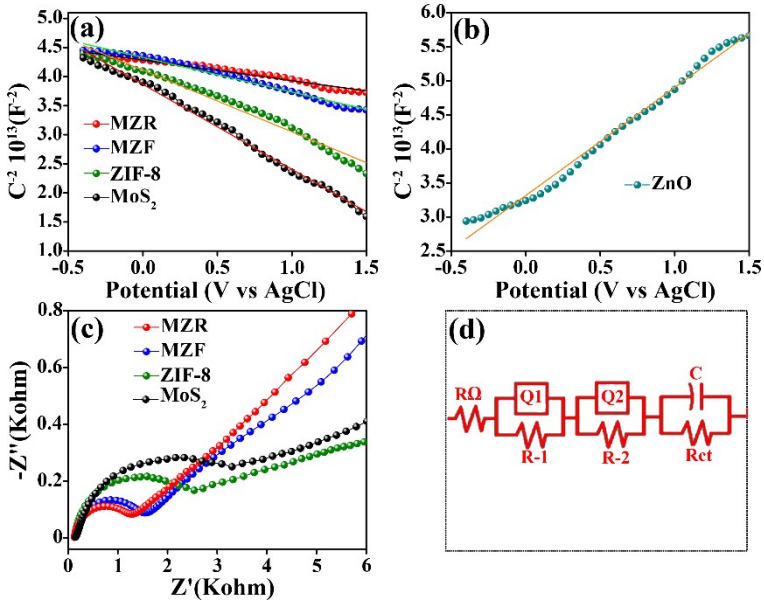

Figure S12. (a) The comparative MS plots of the pristine MoS_2 NSs, ZIF-8, with MZF and MZR; (b) MS plot of pure ZnO; (c, d) Nyquist plots of the composites compared with bare MoS_2 and ZIF-8; (d) equivalent circuit model (Measurement in the solution of 5 mM $Fe(CN)_6^{3-/4-}$containing 0.1 M KCl).

The electrochemical impedance spectroscopy (EIS) was performed by using CHI660E series electro-chemical workstation (Shanghai Chenhua Instrument Co., Ltd., China), with a three-electrode system. The working electrode is glass carbon electrode (GCE) coating with the as-synthesized samples. A silver/silver chloride (Ag/AgCl) served as reference electrode and platinum (Pt) sheet was used as a counter electrode. All three electrodes were vertically immersed in a solution of 5 mM $Fe(CN)_6^{3-/4-}$ (1:1) containing 0.1 M KCl to analyze the electrochemical performance of the modified electrode as shown in Figure S10 c. The testing frequency ranges from 10^3 to 0.1 Hz at 10-mV amplitude.

Table S3. Fitted impedance parameters of the samples.

Samples	MoS_2	ZIF-8	MZR	MZF
R_Ω（Ω）	1109.2	988.1	**693.3**	727.8
R_{ct}（Ω）	10004	8504	**4257**	6731

Table S4. Comparative gas sensing performance of MoS_2@ZnO heterostructure with reported work

Sensing materials	NO_2 (ppm)	Temp. (°C)	Response	t_{res}/t_{rec} (s)	LOD (ppm)	Synthesis technique	Refs.
MoS_2 hollow sphere	100	150	40.5%	79/225	0.5	hydrothermal method	[1]
Exfoliated MoS_2	1.0	200	5.80	2460/2340	0.02	Chemical Exfoliation	[2]
2D MoS_2	50	RT	300%	180/480	25	chemical vapor deposition	[3]
Mixed MoS_2 flakes	10	RT/UV	10.36%	8.51/---	10	chemical vapor deposition technique	[4]
MoS_2/ZnO	50	200	31.2%	---/---	0.2	Sputtering	[5]
MoS_2/SnO_2	5	RT	18.7	---/---	0.25	Hydrolysis process	[6]
MoS_2/ZnO	5	RT	3050%	40/1000	0.05	Wet chemical route	[7]
MoS_2/ZnO	0.2	RT/N_2 (UV)	188%	---/---	0.05	Sonication	[8]
MoS_2/MoO_3	10	RT	33.6%	19/---	10	vapor deposition process	[9]
MoS_2/SnO_2	10	RT	~ 29 %	408/162	0.5	Chemical Exfoliation/ Annealing	[10]
ZnSe/ZnO	8	200	10.42	98/141	1.0	Thermal Oxidation	[11]
ZnO/rGO	2.5	110	33.11	182/234	0.05	Solvothermal method	[12]
rGO-ZnO	5	80	1.26	165/499	1.0	Thermal stirring	[13]

nanoparticles							
ZnO/rGO nanowalls	5	RT/UV	3.5	25/15	5.0	Thermal reduction/soft solution process	[14]
MoS_2@ZnO heterostructure	50	RT	34.91	1.5/30.9	0.01	Ultrasonic/ Hydrothermal process	Present work

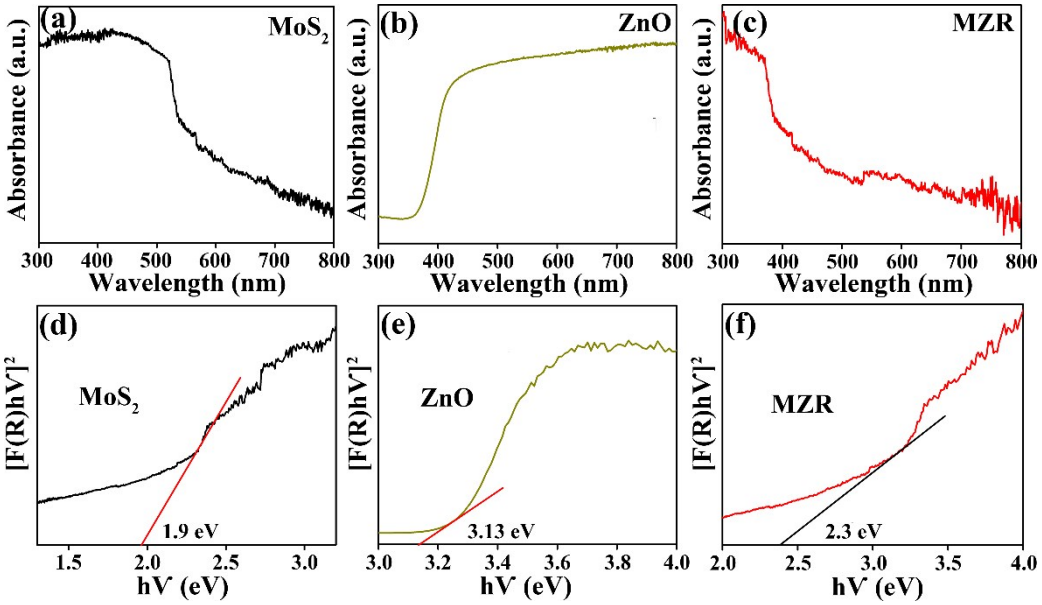

Figure S13. (a-c) UV visible diffused refelectance spectra and (d-f) corresponding plots of transformed Kubelka-Munk verses the energy light of the samples.

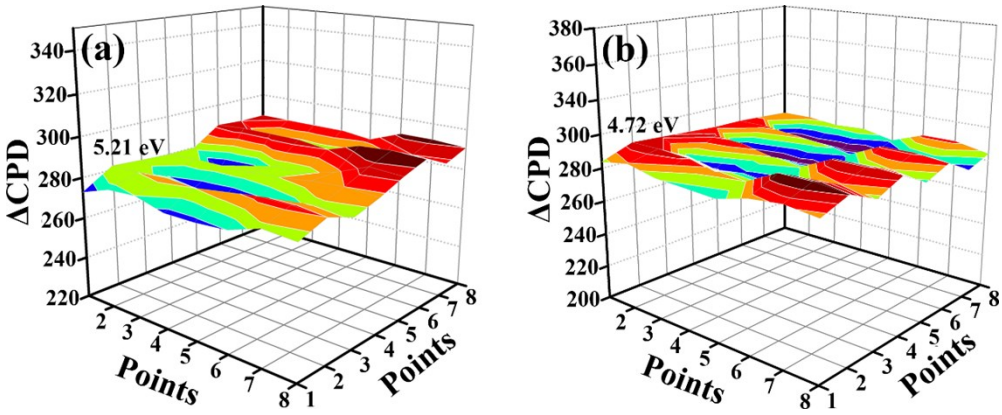

Figure S14. Kelvin probe of (a) MoS_2 NSs, and (b) ZnO rods.

References

1. Y. Li, Z. Song, Y. Li, S. Chen, S. Li, Y. Li, H. Wang and Z. Wang, *Sens. Actuators, B*, 2019**, 282**, 259-267.

2. M. Donarelli, S. Prezioso, F. Perrozzi, F. Bisti, M. Nardone, L. Giancaterini and C. Cantalini, L. Ottaviano, *Sens. Actuators, B*, 2015, **207**, 602-613.

3. Y. Zhao, J. G. Song, G. H. Ryu, K. Y. Ko, W. J. Woo, Y. Kim, D. Kim, J. H. Lim, S. Lee, Z. Lee, J. Park and H. Kim, *Nanoscale,* 2018, **10**, 9338-9345.

4. A. V. Agrawal, R. Kumar, S. Venkatesan, A. Zakhidov, G. Yang, J. Bao, M. Kumar and M. Kumar, *ACS Sens.* 2018, **3**, 998-1004.

5. S. Zhao, G. Wang, J. Liao, S. Lv, Z. Zhu and Z. Li, *Appl. Surf. Sci.,* 2018, **456**, 808-816.

6. Y. Han, Y. Ma, Y. Liu, S. Xu, X. Chen, M. Zeng, N. Hu, Y. Su, Z. Zhou and Z. Yang, *Appl. Surf. Sci.,* 2019**, 493**, 613-619.

7. Y. Han, D. Huang, Y. Ma, G. He, J. Hu, J. Zhang, N. Hu, Y. Su, Z. Zhou, Y. Zhang and Z. Yang, *ACS Appl. Mater. Interfaces,* 2018, **10**, 22640-22649.

8. Y. Zhou, C. Gao and Y. Guo, *Journal of Materials Chemistry A,* 2018, **6**, 10286-10296.

9. R. Kumar, N. Goel, M. Mishra, G. Gupta, M. Fanetti, M. Valant and M. Kumar, *Adv. Mater. Interfaces,* 2018, **5**, 1800071.

10. S. Cui, Z. Wen, X. Huang, J. Chang and J. Chen, *Small* 2015, **11**, 2305-2313.

11. W. Liu, D. Gu and X. Li, *ACS Appl. Mater. Interfaces,* 2019, **11**, 29029-29040.

12. P. Cao, Y. Cai, D. Pawar, S. T. Navale, C. N. Rao, S. Han, W. Xu, M. Fang, X. Liu, Y. Zeng, W. Liu, D. Zhu and Y. Lu, *Chem. Eng. Journal,* 2020, **401**, 125491.

13. S. Liu, B. Yu, H. Zhang, T. Fei and T. Zhang, *Sens. Actuators, B*, 2014, **202**, 272-278.

14. Z. Liu, L. Yu, F. Guo, S. Liu, L. Qi, M. Shan and X. Fan, *Appl. Surf. Sci.,* 2017, **423**, 721-727.